

Processing, structure and properties of alumina-YAG eutectic composites

T.A. Parthasarathy*, T. Mah and L.E. Matson

Air Force Research Laboratory, Materials and Manufacturing Directorate, AFRL/MLLN, Wright-Patterson AFB, OH 45433-7817

Research over the past 15 years on alumina-YAG eutectic composites as a high temperature structural material is reviewed. It is suggested that this is among the most attractive oxidation-resistant systems for ultra high temperature (1500 °C) structural use. Processing methods studied to date result in alumina-YAG composites of varying length scales of constituent phases ranging from micrometers down to nanometers. Variations in constituent geometry from bulk eutectics to fibers and powders have been explored. The microstructures have ranged from single crystal eutectics with both coarse and fine eutectic structures to polycrystalline eutectics. The properties of interest are strength at temperature, creep resistance, fracture toughness and environmental stability. High temperature strength has been found promising and the creep resistance is among the best in oxide ceramics and is sufficient for applications up to 1500 °C. The mechanisms of creep have been studied extensively. The fracture resistance continues to be less than desired for most structural applications. The effect of dopants on the fracture behavior has shown some promise, but there has not been a systematic study and is suggested for future work. This system has excellent environmental stability in a combustion environment compared to other high temperature structural solids.

Key words: Alumina, YAG, eutectic, review, processing, structure, properties.

Introduction

The increase in thermal efficiency with use temperature and the increased demand for higher performance in aircraft and spacecraft applications have both demanded structural materials that can survive higher temperatures. The state of the art nickel-based superalloys can be used at metal temperatures of up to nearly 1100 °C; the thermal barrier coatings allow their use at gas temperatures that are 100 °C higher. Ceramic materials offer the potential for higher temperatures of operation with lower density and higher modulus. The most attractive ceramic composites are at present based on fibers of carbon or silicon carbide. While these composites have shown remarkable performance, their oxidation resistance is still limited at temperatures above 1200 °C, especially in a moisture-containing combustion environment. For long-term use at temperatures above 1200 °C, oxide ceramics have the inherent advantage of stability against oxidation. In addition to lack of oxidation issues, ceramics based on alumina and rare-earth oxides show resistance to attack by moisture, which the non-oxides are prone to at higher temperatures and pressures. The oxidation-resistant oxide-oxide composites at present rely on polycrystalline oxide fibers, which are limited in creep above 1200 °C. Thus single crystal

oxides are required for ultra-high temperature use in oxidizing environment. Composites reinforced with single crystal fibers have not been attractive due to the expense of fabricating single crystal oxide fibers. The low cost processing of in-situ composites using an eutectic reaction is quite attractive. Eutectic oxides thus show the most promise for applications requiring ultra-high temperature structural materials. The alumina-YAG eutectic system was identified as an ultra-high temperature structural material by Mah *et al.* [1] and Parthasarathy *et al.* [2, 3] Several studies in the past decade have confirmed the superior mechanical properties of this eutectic system at ultra-high temperatures (at and above 1400 °C) [4-19].

Simultaneous to these developments, a survey of the creep resistance of single crystal oxides was performed by Corman [20]. In addition, this work included a comparative study of the most promising oxides in single crystal form [20, 21]. This study showed that among the oxides whose creep behavior was known till then, Yttrium Aluminum Garnet (YAG) was significantly better than all other oxides. Since then, several studies on YAG have been conducted which confirm the high creep resistance of this material, which is believed in part due to the large lattice parameter and hence large Burgers vector of the dislocations [3, 22-26].

From the above, it is clear that among the oxide eutectics, those that employ YAG as one of the constituents are likely to have the best creep resistance and thus the most promising as ultra-high temperature structural material. Alumina is an obvious choice due

*Corresponding author:
Tel : +1-937-255-9809
Fax: +1-937-255-3007
E-mail: Triplicane.Parthasarathy@wpafb.af.mil

to the stable eutectic that it forms with YAG [27]. However several other criteria must be met before a system is considered for structural use. First, the two constituents must be chemically stable to offer microstructural stability during use. Second, the two must have similar thermal expansion coefficients to minimize processing stresses. Third they must be resistant to environmental attack including moisture. Fourth they must resist vaporization under low oxygen partial pressure conditions. Fifth the two constituents must exhibit no phase changes up to the melting point. Finally, for ease of processing, they must form a eutectic that will allow melt processing. From the various possible systems, the eutectic of alumina and YAG emerged as the most promising [1-3]. This system was studied over the past decade by several investigators and it continues to be one of the most attractive ultra-high temperature composite systems. This paper is a review of the work on this system.

The paper is organized as follows. A brief history of the early studies leading to the phase diagram of this system is presented first. This is followed by recent studies where the focus has been on developing the alumina-YAG eutectic as a high temperature structural system. The recent work is classified into three sections, namely processing, microstructures and properties. In the processing section, the processing of bulk eutectics, fibers of the eutectic and polycrystal eutectics are covered. In the microstructures section, the variability in microstructure in the as-processed conditions as well as heat treated conditions are presented. In the last section, the strength, creep and toughness of these materials are covered. The paper ends with suggestions for future work.

Phase Diagram

The phase diagram of the Alumina-Yttria system as known today is due to the works of Warsaw and Roy [28], Viechnicki and Schmid [29], Caslavsky and Viechnicki [30], and Mah and Petry [31]. One of the earliest studies on this system, by Warsaw and Roy [28] established the eutectic reactions in the alumina-yttria system. The phases alumina and YAG were reported to form a eutectic at 1760 °C. The perovskite phase was suggested to be metastable and hence is missing in the first phase diagram. This work was followed up by Viechnicki and Schmid [29] who found the eutectic temperature to be 1800 °C and the eutectic composition to be 18.7 mol% Y_2O_3 and 81.3 mol% Al_2O_3 . This work was the first to report on the microstructures of the Alumina-YAG eutectic (AYE) grown using the Bridgman crystal growth technique. Under certain processing conditions (1850 °C, 190 °C/cm, 4 cm/hr), they obtained an oriented eutectic microstructure. Nearly a decade later, Caslavsky and Viechnicki [30] conducted exhaustive studies to confirm the melting

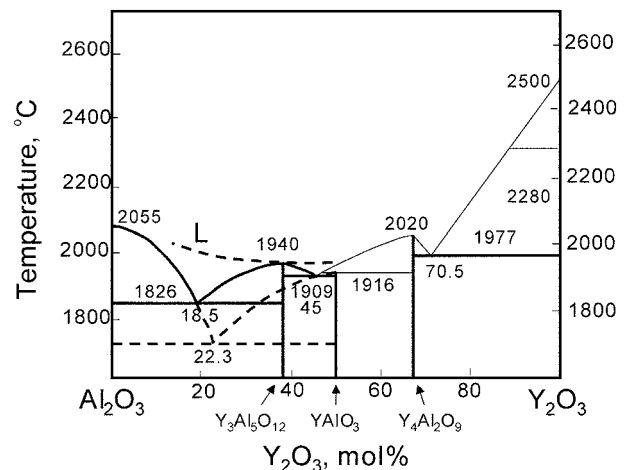


Fig. 1. The equilibrium phase diagram of the Alumina-yttria system derived from the works of Warsaw and Roy [28], Caslavsky and Viechnicki [30] and Mah and Petry [31]. The dotted lines show the metastable eutectic formation when the melt temperature of compositions in the range ~10-45 mol% Y_2O_3 exceeds that given by the dotted line in the liquid phase marked 'L'.

point of YAG to be 1940 °C ± 17 °C. In addition, they presented the first complete phase diagram that included the perovskite phase. They presented the metastable eutectic reaction at 1702 °C ± 7 °C and 23 mol% Y_2O_3 -77 mol% Al_2O_3 . They further reported the formation of the stable YAG phase from this metastable eutectic at 1418 °C ± 7 °C. Finally, they made the most intriguing observation that when the melt temperatures do not exceed 1940 °C, melts of composition ranging from 10 to 45 mol% Y_2O_3 , retain aluminum in the 4-fold coordination and thus obey the equilibrium phase diagram upon cooling. On the other hand, if the melt temperature exceeds 2000 °C, they reported that the melt changes to a 6-fold coordination for Al, thus favoring the metastable eutectic reaction upon cooling. This was later confirmed by Mah *et al.* [27]. Hay [32] and most recently by Yasuda *et al.* [33, 34]. The phase diagram as inferred from the works of Warsaw and Roy [28], Viechnicki and Schmid [30] and Mah and Petry [31] is shown in Figure 1. In Fig. 1, the solid lines refer to the equilibrium phase diagram, while the dotted lines refer to the metastable eutectic reaction that occurs upon cooling, when the melt temperature exceeds the liquidus given by the dotted line.

Processing of In-situ (Eutectic) Composites

For a comprehensive review of directional solidification of ceramic eutectics see the works of Ashbrook [35] and Stubican and Bradt [36]. The latter study refers to the processing of oxide eutectics in the alumina-YAG system by Viechnicki and Schmid [29] mentioned earlier but no further details on the processing aspects of this eutectic system can be found. From theoretical considerations, Stubican and Bradt predict a lamellar (as against rod-like) microstructure for directionally

solidified alumina-YAG.

The first reported study on the processing of significant quantities of directionally solidified alumina-YAG eutectic for mechanical property assessment as a potential high temperature structural material was by Mah, Parthasarathy and Matson [1]. This choice was based on a combination of literature review and selected experimental studies of potential eutectic systems [27]. Based on several factors including chemical stability, negligible solid solubility (thermal stability), resistance to combustion environment (including moisture), high melting point, thermo-mechanical compatibility and creep resistance, they determined the alumina-YAG system to be the most attractive for high temperature ($>1200\text{ }^{\circ}\text{C}$) structural applications [27]. It is worth noting that a later work of Li and Bradt [37] identified that alumina and YAG form a significantly better thermo-mechanical match than alumina and mullite, the only other creep resistant oxide comparable to YAG as shown by Corman [21]. Low residual stresses consistent with the

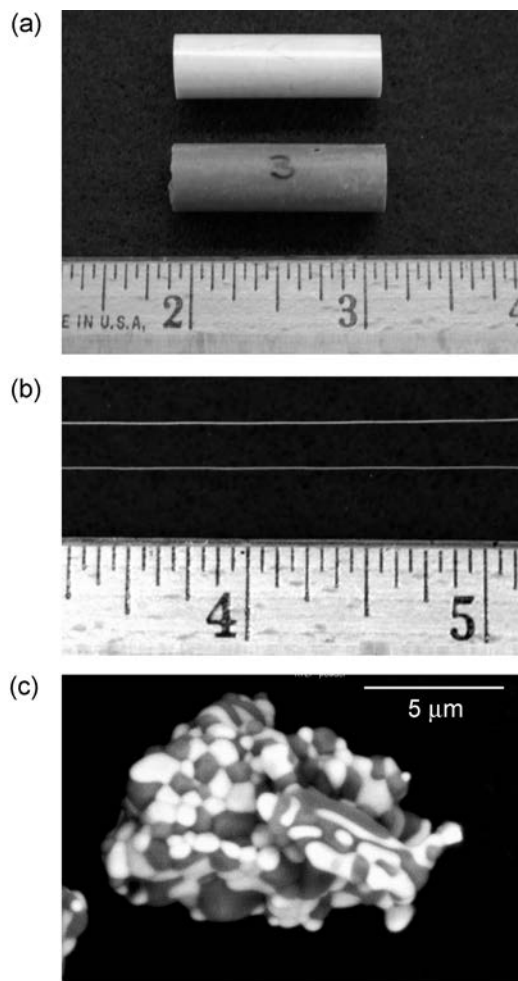


Fig. 2. Different forms in which alumina-YAG eutectics can be fabricated (a) bulk directionally solidified eutectic made using the process sketched in Fig. 3. (b) Long continuous fibers of the eutectic fabricated using the EFG method shown in Fig. 4(a). (c) powders of alumina-YAG eutectic made using the process sketched in Fig. 5(a).

predictions of Li and Bradt were measured in a recent study by Dickey *et al.* [38].

The alumina-YAG eutectic has been fabricated in three different forms, (a) bulk directionally solidified eutectic, (b) fibers of the eutectic, and (c) powders of eutectic consolidated in to a polycrystal. These three forms are shown in Figure 2. The processing methods for these three types are discussed separately.

Bulk Directionally Solidified Eutectics

Mah *et al.* [1, 27] used a modified Bridgman-type crystal growing technique to grow alumina-YAG eutectic composites using a 3/8" (9.6 mm) i.d. molybdenum tube as a crucible. A graphite susceptor inside an induction coil was used as heat source to obtain a short heating zone, with the capacity to reach $2300\text{ }^{\circ}\text{C}$. Presintered mixture of alumina and yttria powders was placed in the crucible and lowered through the hot zone at a controlled rate to effect desired solidification rates. The crystals were grown under an Argon atmosphere at rates of 2-6 cm/hr. A schematic of the processing method is shown in Fig. 3.

Using this process bulk eutectic crystals that were 3/8" (9.6 mm) in diameter and several tens of millimeters long could be fabricated (as in Fig. 2a). Preliminary work confirmed the transition from alumina-YAP eutectic to alumina-YAG eutectic as the melt temperature was increased, as previously shown by Caslavsky and Viechnicki [30] The alumina-YAP eutectics readily formed aligned rod-like microstructures, which might have advantages in properties, while the microstructure of alumina-YAG eutectics showed a "Chinese-script" morphology, which might offer more isotropic properties. However the instability of YAP with alumina precludes the use of alumina-YAP eutectics for high temperature use. Several studies have explored the effects of

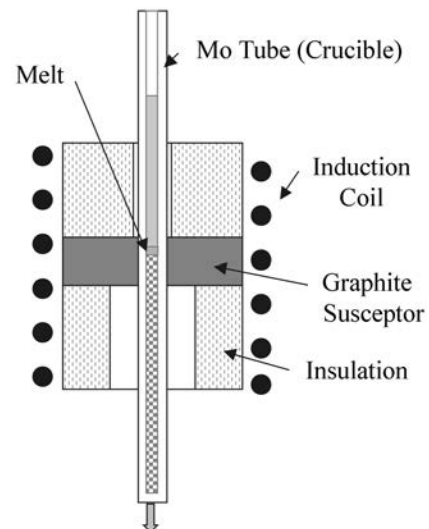


Fig. 3. A modified Bridgman-type crystal growth apparatus used to fabricate bulk eutectic crystals of alumina-YAG eutectic composites (Mah *et al.* [1, 27]).

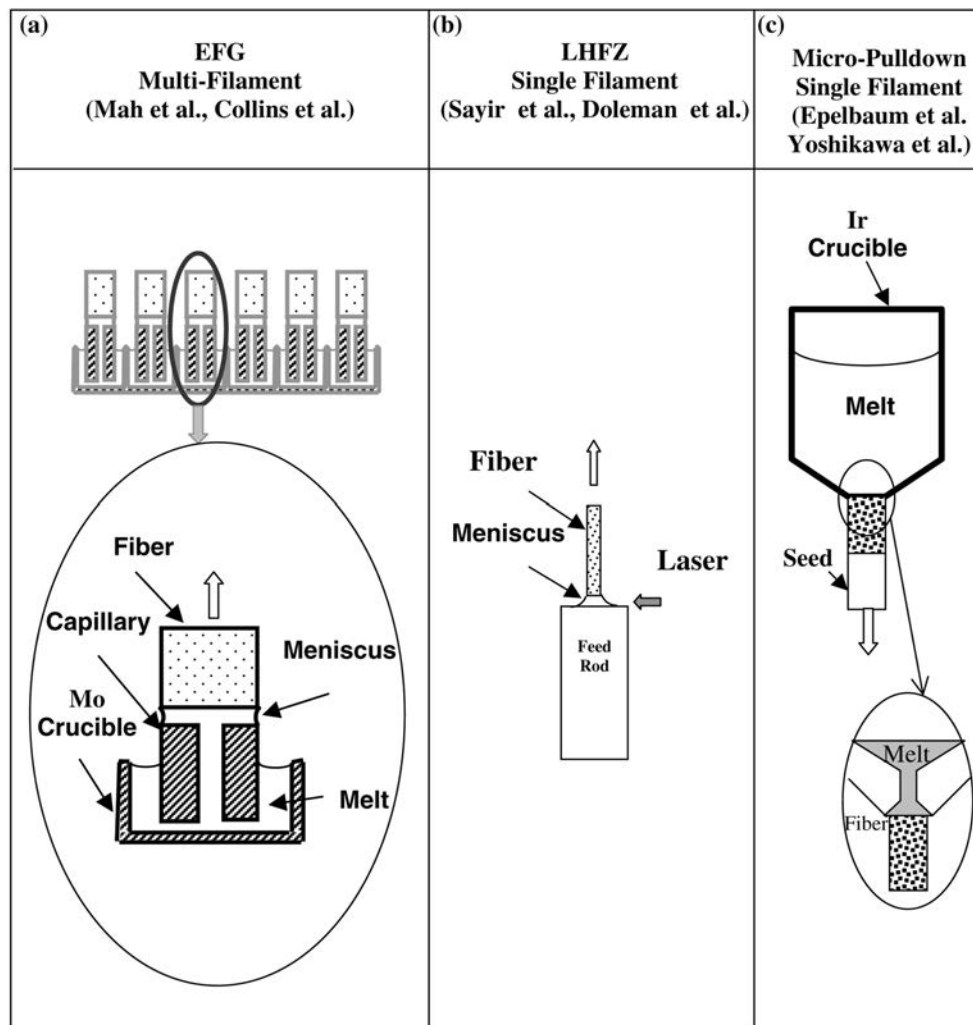


Fig. 4. Schematic sketches of the three processes reported in the literature for fabricating fibers of eutectic composites. (a) film fed Edge-Defined-Growth (EFG) processing method (Mah *et al.* [5], Collins *et al.* [58]) and (b) Laser-Heated Float Zone (LHFZ) method (Sayir *et al.* [43, 44, 60]. Doleman and Butler [45]) and (c) Micro Pull-down method of Epelbaum *et al.* [46] and Yoshikawa *et al.* [13]

processing variables on the solidification of this system [34, 39–42], confirming the curious solidification pathways mentioned earlier and in one interesting study using this phenomenon to fabricate complex shapes [42].

Eutectic Fibers

The advances in continuous fiber reinforced ceramic composites using Nicalon™ and other SiC-based fibers motivated interest in developing an oxide analogue for use in an oxidizing environment. The poor creep resistance of oxides in fine grain polycrystal form pointed towards single crystal oxide fibers for ultra-high temperature structural use. Sapphire was the only single crystal oxide fiber available; but it had the disadvantage of loss in strength with temperature and high anisotropy in creep. The high strength retention of the bulk eutectics up to very high (1400 °C) temperatures and the high creep strength of YAG motivated the work on fabricating the eutectic in the fiber form.

Three different processing methods have been reported

in the literature for growing alumina-YAG eutectic fibers. These are (1) the film-fed Edge-Defined-Growth (EFG) technique [5, 6] (2) the Laser-Heated Float Zone (LHFZ) [43–45] growth process and (3) the micro pull-down method [13, 46]. Schematic sketches of the three processing methods are shown in Fig. 4. The EFG method is typically run using multiple capillaries to obtain multifilaments from a single die and thus is the most cost-effective. The EFG technique was used to grow alumina-YAG eutectic fibers by Mah *et al.* [5, 6] using molybdenum crucibles and capillaries. These fibers are grown from a charge of the constituent powders melted in a crucible with capillaries that allow the melt to rise up the capillary to an orifice whose shape defines the cross-sectional shape and size of the crystal grown. Continuous spooled fibers of diameters ranging from 75 to 150 micrometers were fabricated at growth rates of 30 to 120 cm/hr using the EFG method by Mah *et al.* [5, 6] (as in Fig. 2b). In the LHFZ, source rods are prepared by extrusion of constituent powders

without presintering. To grow a single crystal of the eutectic, a seed of single crystal alumina is used and crystals have been grown at rates of the order of 40 cm/hr. Eutectic fibers of diameters 150 to 250 micrometers and lengths of 30-50 cm have been grown by Sayir and Matson [4]. The LHFZ provides the ease of fabricating novel compositions for microstructural evaluation and some mechanical property determination. In a recent study, a micro-pull down method was developed with very high pulling rates (up to 10 mm/minute) with essentially the same results as the other two methods in terms of microstructures obtainable [13, 46]. The method uses an iridium crucible containing the melt, with the fiber being pulled out from the bottom as shown in Fig. 4c. The method shows promise as a high rate fiber fabrication method.

Polycrystal Eutectics

The most recent studies have focused on the fabrication of alumina-YAG polycrystal eutectics [47-49]. The polycrystal eutectics are attractive since they offer the potential for high strength and creep strength, since the eutectic scale is believed to determine both the fracture strength and creep strength, rather than the grain size, allowing large grained, creep resistant polycrystals of high strength possible. Both of the reported studies use mechanical crushing and attrition of melt-formed

alumina-YAG eutectic to obtain eutectic powders (as in Fig. 2c). In the long term, atomization techniques are envisioned for obtaining large scale powder fabrication. Schematics of the process methods studied thus far are shown in Figure 5. The powder was consolidated by Mah *et al.* [47] using hot-pressing while Isobe *et al.* [48] used spark plasma sintering (SPS). Mah *et al.* used powders sieved to less than 150 micrometers, and hot pressed at 1600°-1700 °C with 20 MPa for 15 minutes. Isobe *et al.* used powders of size 3-44 and 64-124 micrometers and consolidated at 1690°-1710 °C, for 20 minutes in vacuum with 20-40 MPa pressure in a graphite die with spark plasma assistance. In both cases polycrystals of the eutectic was successfully fabricated to near theoretical density, with no significant coarsening of the eutectic microstructure.

Microstructure and Its Stability

The microstructures of directionally solidified alumina-YAG eutectic composites exhibit a significant variation depending on the processing history. The analysis of Stubican and Bradt [36] predicted that the alumina-YAG eutectic will grow as a lamellar structure. Unfortunately the alumina-YAG system under directional solidification exhibits a irregular-script-type morphology under most conditions. The early work of Viechinicki and Schmid [29] showed that it was possible to obtain an aligned microstructure with a gradient of 190 °C/cm and growth rate of 4 cm/hr. However, even under this condition the structure was a mixture of rods and platelets indicating that the planarity of the liquid/solid interface tended to break down often. The most comprehensive work on the effect of process variables on the microstructural scale and morphology is the recent work by Mizutani *et al.* [40, 41]; they evaluated the process window within the Bridgman technique to obtain coupled growth and found it to be narrow. Further they found that planar solidification did not occur even at growth rates of 10^{-7} m/s; however the microstructural scale did follow the well known inverse square-root dependence on growth rate. The same results were shown by Epelbaum *et al.* [46] using a micro-pull down method which could be used to produce fibers at pulling rates up to 10 mm/minute.

The microstructure of a directionally solidified bulk alumina-YAG eutectic, grown using the modified Bridgman technique (shown in Fig. 3), is shown in Figure 6a. The microstructure was taken under secondary electron imaging mode in an SEM; the lighter phase is YAG and the darker phase is alumina. The volume fraction of the YAG phase was measured to be 45%, which is close to that predicted by the phase diagram. Columnar colonies that align along the solidification direction are seen, along with a tendency for the YAG phase to be longer along the growth direction by a factor of 2 to 3, but the structure shows no evidence for

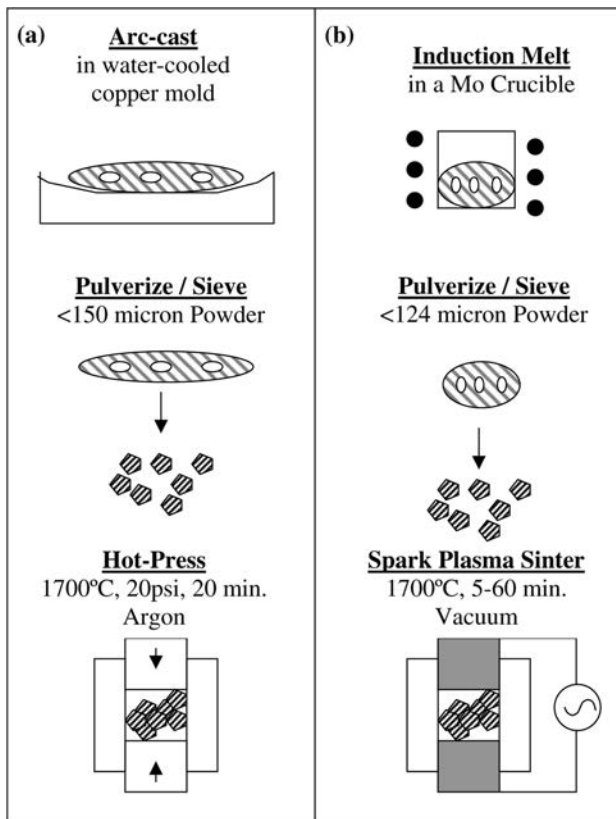


Fig. 5. Schematic sketch describing the process used to fabricate alumina-YAG eutectic by (a) Mah *et al.* [47] and (b) Isobe *et al.* [49].

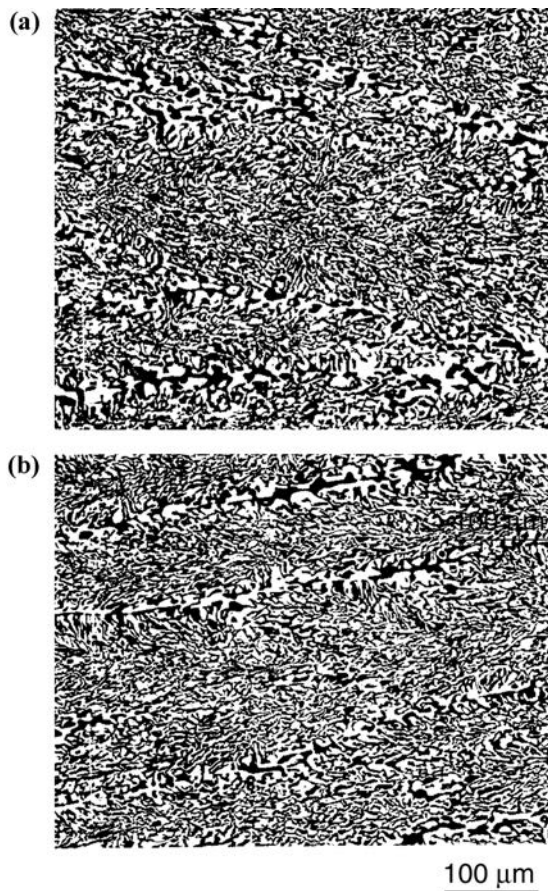


Fig. 6. Microstructures of the alumina-YAG eutectic directionally solidified using a modified Bridgman technique (Fig. 3) in (a) the as-solidified condition and (b) after a heat treatment in air for 5 hrs at 1700 °C. The eutectic is seen to exhibit excellent thermal stability at this temperature (Mah *et al.* [1]).

coupled growth. The distribution and the volume fraction imply that the composite is co-continuous, but with facets. A detailed TEM investigation of the structure can be found in the work by Hay *et al.* [50-52]. A regular orientation relationship between the alumina and the YAG phase was confirmed from these studies, despite the decoupled growth during solidification. These investigations and X-ray diffraction studies of the directionally solidified eutectics [2, 22, 53] showed that the microstructure of these materials consists of a co-continuous mixture of a single crystal of alumina and a single crystal of YAG. Thus the microstructure is a unique in-situ composite with both the matrix and reinforcement made of single crystals. The stability of these alumina-YAG microstructures has been demonstrated in many studies. Mah *et al.* [27] showed that a heat treatment in air for 5 hrs at 1700 °C caused no significant coarsening (Fig. 6b). Several studies have confirmed the inherent stability of this system [12, 18, 54-57].

The microstructure of this eutectic was further refined first by Mah *et al.* [5] and later by Collins [58] and Matson and Necht¹² using the EFG process. The

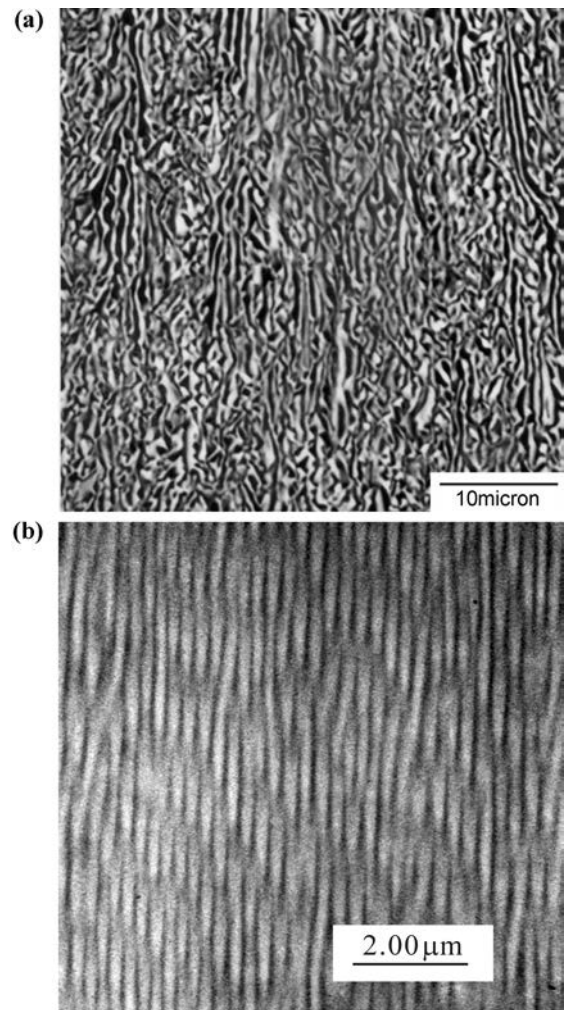


Fig. 7. Microstructures of the alumina-YAG eutectic fibers fabricated using the EFG process (Fig. 4a) by (a) early work of Mah *et al.* [5], at 0.5 in/minute (12.7 mm/minute) pulling rate and (b) later work by Matson and Hecht [12] at 1 in/minute (25.4 mm/minute). The growth direction is vertical in both cases. The microstructure shown in (b) was observed only within a fraction of the fiber cross-section and not the entire section.

microstructures of fibers grown using this process are shown in Figure 7. It is seen that highly aligned microstructures can be obtained when the size of the grown crystal is small (~75 micrometers); however detailed analysis of the structure shows that this highly aligned structure is limited to only a portion of the grown fiber and is not retained across the entire width of the fiber [12]. Similar results were obtained on directionally solidified fibers grown using the LHFZ method [44, 59, 60]. Using specimens from these fibers, Frazer *et al.* [44] confirmed the orientation relationships between alumina and YAG over a wider spatial range than the study of Hay and Matson [51]. They also reported the variation in microstructural scale from the surface to the interior of the fiber, finer on the outside and coarser inside.

The microstructures of the polycrystal eutectic fabricated using the processes shown in Fig. 5 are shown

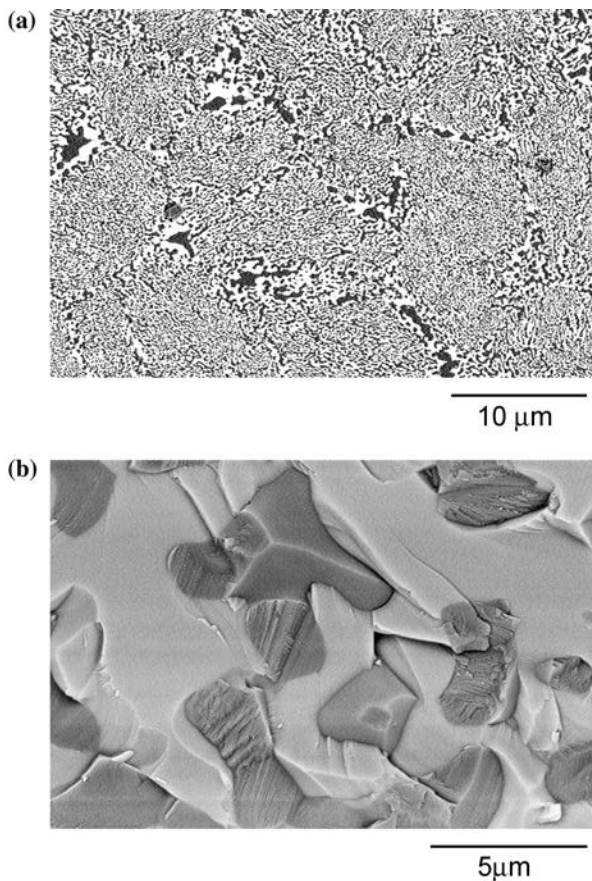


Fig. 8. SEM Microstructures of the alumina-YAG polycrystal eutectic obtained using the processing method shown in Fig. 5. (a) Polycrystals with grains that are nearly 50-100 micrometers in size fabricated by Mah *et al.* [47] using hot-pressing of powders obtained by crushing arc-cast eutectic and sieving to <150 micrometer sized particles (see Fig. 5a). The eutectic structure is seen to be maintained after consolidation with little coarsening (compare with structures in Fig. 6). (b) shows the fractured surface of a doped polycrystal eutectic showing the possibility of weakening the interface between the two phases for enhancing fracture toughness [69].

in Fig. 8. Hot-pressing resulted in good retention of the microstructure of the as-cast eutectic, while the spark plasma sintering (SPS) process was reported to result in additional formation of new crystals [49]. In particular note that the microstructural scale is nearly the same as the directionally solidified bulk eutectics shown in Fig. 5, confirming the high thermal stability of the microstructure against reaction or coarsening. During SPS it is possible that local temperatures exceeded the melting point and caused nucleation of fresh grains.

Mechanical Properties

The mechanical properties of the alumina-YAG eutectics were first measured on directionally solidified bulk eutectics by Mah *et al.* [1] and Parthasarathy *et al.* [2] Later studies focused on the strength and creep resistance of fibers. More recently, the strengths of the polycrystalline eutectic have been reported. Data on

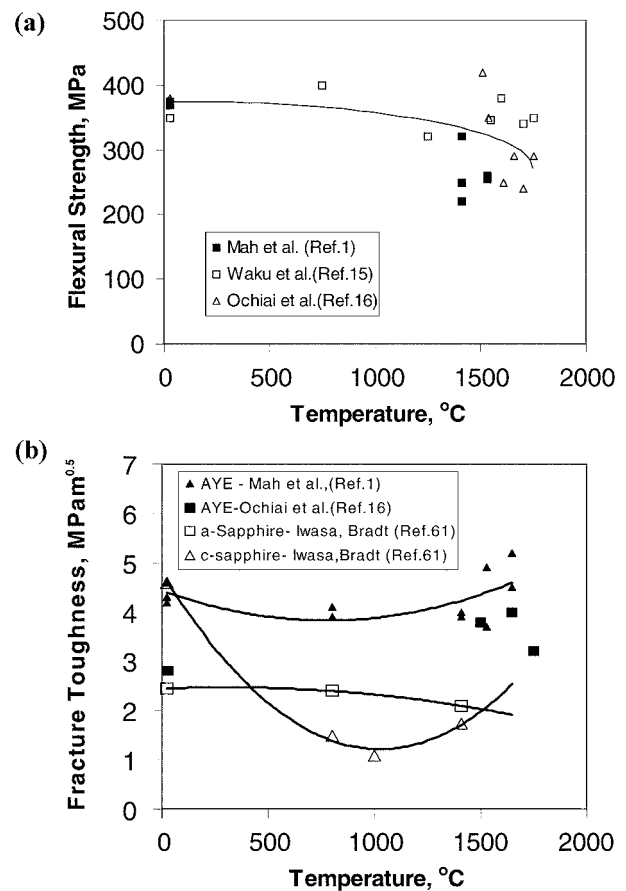


Fig. 9. The flexural strength and fracture toughness of directionally solidified bulk alumina-YAG eutectic are shown plotted as a function of temperature. (a) The flexural strength is shown retained to 1500C. (data from Mah *et al.* [1], and Waku *et al.* [15, 16]) (b) fracture toughness is also retained up to 1500C, with toughness being better than its constituents. (AYE data from Mah *et al.* [1, 76], and Ochiai *et al.* [16] sapphire data from Isawa and Bradt [61], YAG data from Mah and Parthasarathy [62]).

these three types of material are presented below; this is followed by a comparative evaluation.

Directionally Solidified Bulk Eutectics

Mah *et al.* [1] and Parthasarathy *et al.* [2] were the first to study the mechanical properties of the alumina-YAG eutectics. They studied the behavior of directionally solidification structures that were essentially a single crystal sapphire co-continuous with a single crystal YAG. Specimens were taken from bulk solids that were 3/8" in diameter and several inches long for mechanical property evaluation. They measured and reported the flexural strength, fracture toughness and creep resistance.

The measured strength and fracture toughness as a function of temperature are shown in Figure 9. The flexural strength was about 300 MPa at room temperature, but with microstructural refinement higher strengths were anticipated. The most important result was that the mechanical strength and fracture toughness are both well retained up to 1500 °C. The fracture toughness values are shown compared with those of sapphire [61]

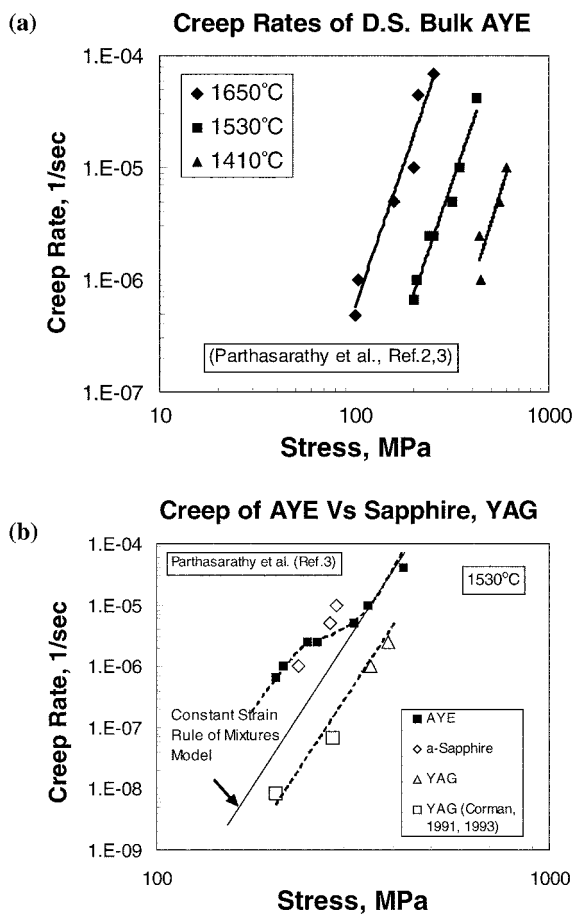


Fig. 10. The measured creep rates of directionally solidified AYE eutectic as reported by the early work of Parthasarathy *et al.* [2, 3] In (b) the AYE behavior is compared with data obtained under the same conditions on single crystals of YAG and α -axis sapphire. They suggested that refining the microstructure with a long aspect ratio of the YAG phase will yield better creep behavior close to the constant strain rule of mixtures model.

and single crystal YAG [62]. It is clear that the eutectic structure exhibits an enhancement in fracture toughness compared to the constituents and that it is retained up to 1600 °C. This was later confirmed by Harada *et al.* [63, 64]. The fracture toughness of the composite, 4.5 MPam^{0.5}, is significantly higher than most monoliths, but still insufficient for most structural applications.

Parthasarathy *et al.* [2, 3], were the first to study the creep resistance of this material at elevated temperatures (1400 °C to 1600 °C). The results obtained on the bulk eutectic are shown in Figure 10(a). In Fig. 10(b), the data at 1530 °C are compared with the creep behavior measured under identical conditions using α -axis sapphire and single crystal YAG. It is seen that the creep strength of this eutectic follows the rule of mixtures (on a constant strain model) at high stresses but is weaker than α -sapphire at lower stresses. This was suggested as due to diffusional relaxation at the YAG-alumina interfaces, and it was predicted that refining the microstructure with a high aspect ratio of the YAG phase would yield better creep resistance. Some evidence for

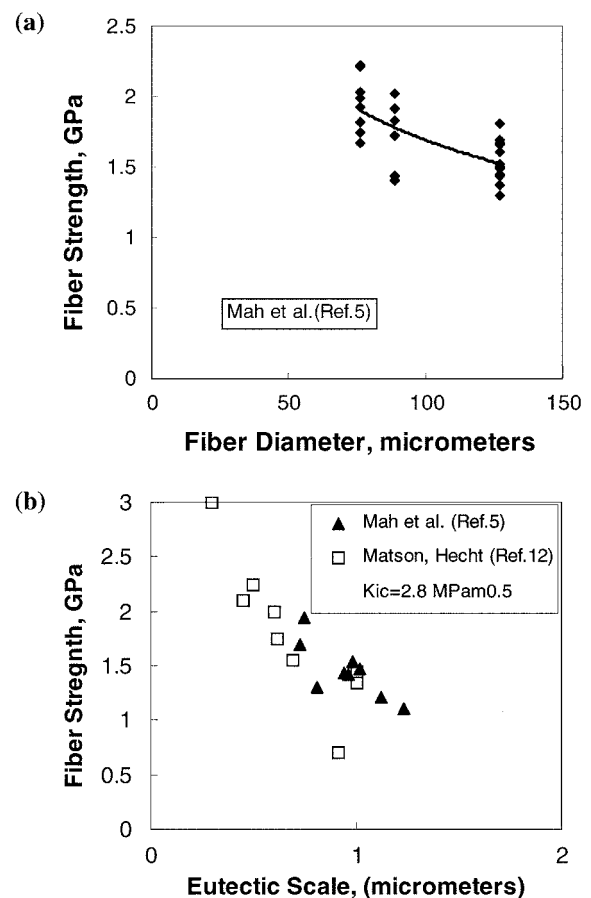


Fig. 11. The strength of alumina-YAG eutectic fibers grown using the EFG process are shown plotted as a function of fiber diameter in (a), redrawn from Mah *et al.* [5] Smaller fiber diameters yield higher strengths as expected. The fibers' strength plotted as a function of the eutectic scale is shown (b) for two batches of grown fibers [5, 12]. It is clear that the strengths of the fibers are limited by the microstructural scale and the dependence on fiber diameter in (a) most likely arises from the same. A fracture toughness of about 2.8 MPam^{0.5} is indicated from these data.

this was reported later by Matson and Hecht [12] using eutectic fibers, which is presented in the next section.

Eutectic Fibers

The interest in the fibrous form of the eutectic stems from the fact that fracture toughness of the bulk eutectic was insufficient for direct use as a structural material. In addition, there was a need for high temperature creep resistant fiber that had high tensile strength. While YAG fibers will form the most creep resistant oxide fibers, they have a low fracture toughness, of the order of 1 MPam^{0.5}, which lowers the maximum possible strength obtainable with them. The eutectic structure offers a significantly higher fracture toughness as seen from Fig. 9, thus offering the possibility of a high temperature creep-resistant fiber with a high fracture strength.

Mah *et al.* [5, 6] were the first to report on the strength of the alumina-YAG eutectic fibers. The strength of EFG-grown fibers are shown in Fig. 11. From Fig. 11a,

it is seen that smaller fiber diameters result in increased strength. Since the effective cooling rate is likely to increase with decrease in diameter, finer eutectic structure and hence higher strength were suggested. A plot of fiber strengths obtained by Mah *et al.*, Collins *et al* [58], and Matson and Hecht [12], is shown in Fig. 11b. It is seen that the strength of the fibers scale with the spacing of the two phases in the microstructure with an inverse square-root dependence, as expected. An effective fracture toughness of 2.8 MPam^{0.5} is obtained from these data. This value is lower than that measured for bulk eutectic using SENB method, shown in Fig. 9.

Creep of the eutectic fibers was studied in detail by Matson and Hecht [12] and the results are summarized in Figure 12. The creep rates of the eutectic fibers grown by EFG process from two different batches and with varying microstructures were studied. The stress dependences could best be described using a threshold stress, which was found to decrease monotonically with

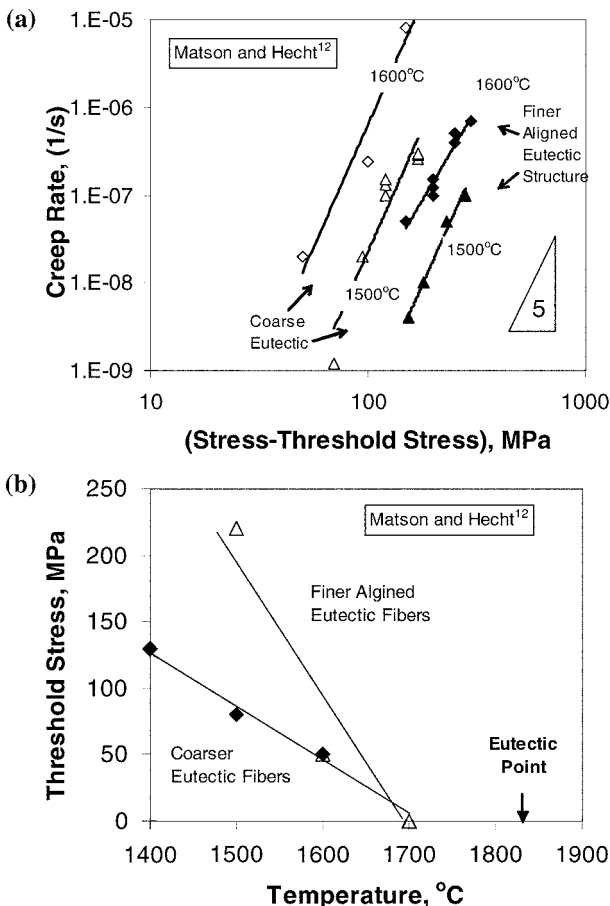


Fig. 12. The creep of eutectic fibers were found to be best described through the use of a threshold stress ($\sim Gb/\lambda$) corresponding to the spacing, λ , of the harder YAG phase. The threshold stress obtained from the measured data decreased with temperature, as expected from the change in shear modulus, G , with temperature. Extrapolation of this decrease with temperature agreed well with the melting point of the eutectic, justifying the concept of using threshold stress to understand the behavior. (redrawn from Matson and Hecht, [12]).

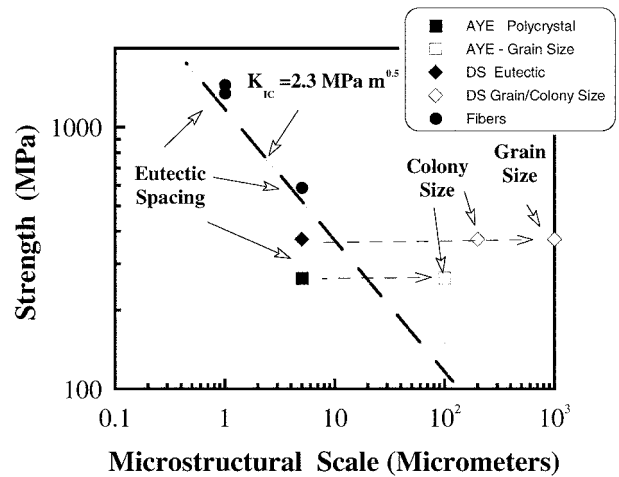


Fig. 13. The variation of strength with microstructural scale is shown plotted for eutectic fibers, bulk eutectic and for polycrystal eutectic. It is seen that the strength dependence is best described by the scale of the two phases in the microstructure than by the fiber diameter, grains size or colony size.

temperature (Fig. 12a). Further an extrapolation of the threshold stress corresponded well with the known melting point of the alumina-YAG eutectic, as shown in Fig. 12b. Several recent studies have explored further details of the creep mechanisms in this system [10, 14-16, 19, 65-67]. These studies support the mechanism to be dislocation creep within alumina with effective load transfer to the creep resistant YAG phase offering creep reinforcement.

Polycrystal Eutectic

The strength of polycrystal eutectics are shown in Figure 13 as a function of microstructural scale. The plot also shows the strength of eutectic fibers as a function of eutectic spacing. It is seen that the polycrystal and bulk eutectic strengths are best described by the dependence on microstructural scale. This plot verifies that the strength of the eutectics in the alumina-YAG system are determined entirely by the eutectic microstructural spacing rather than by the fiber diameter, grain size or colony size.

Limitations and Future Directions

In this review, the alumina-YAG eutectic composite has been argued to be the most promising structural material for ultra-high temperature use in oxidizing environments including those containing significant amounts of moisture. This is based on the microstructural stability, environmental stability, strength retention at temperatures above 1500 °C, excellent creep resistance, and processibility. The attractiveness of the system is easily seen by a comparison of creep behavior of this eutectic with other engineering high temperature materials, shown in Fig. 14. Significant improvements in creep resistance above these values have appeared in

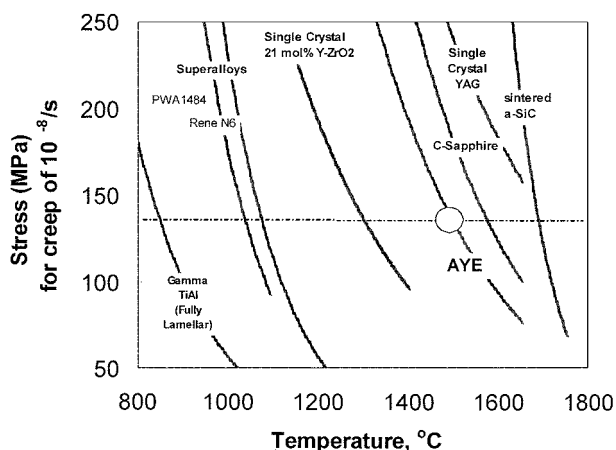


Fig. 14. The creep stress for a creep rate of 10^{-8} /sec (1% in 300 hrs) are shown compared for a variety of engineering materials along with that of Alumina-YAG eutectic composite. The data were obtained from various sources: Gamma TiAl [77] superalloys [78, 79], polycrystal YAG [23], single crystal 21 mol% Y-ZrO₂, [80] AYE [3], sapphire [3, 81], single crystal YAG [3, 21] and SiC [82]. The horizontal line represents the use temperature in aircraft engine applications, based on the current use temperature of the superalloys. The plot shows that alumina-YAG composite is the preferred material for up to 1500 °C application, if oxidation, fracture toughness and environmental resistance are included in the consideration.

a recent work [19]. Despite these attractive features, one key property has continued to plague this system. The fracture toughness of this system is better than the constituents and is comparable to the most tough monolithics, but still too low for engineering use. However there exists a significant potential to increase the fracture toughness of this system. Early work showed that dopants such as strontium might segregate to the alumina-YAG interfaces and weaken them, providing for enhancements in fracture toughness through crack deflection mechanisms [68]. Preliminary work conducted on eutectic polycrystals has shown promise [69]. Other studies have shown significant effects of dopants on fracture behavior and toughness [70, 71]. However there has not been any significant work that studied the effect of a variety of dopants in a systematic way. This is suggested as future work that holds the key to transitioning this material to applications.

Recent works have also extended the alumina-YAG eutectic concept to other eutectics that form between alumina and other rare-earth garnets. In particular, the alumina-gadolinium oxide system has shown promise with respect to high temperature strength and fracture toughness [72, 73]. High creep resistance has been noted in the Alumina-Erbium oxide system [73-75].

Summary

Research over the past decade on the alumina-YAG eutectic system is reviewed. This system shows a very high potential for use as structural material at

temperatures above 1200 °C, and up to 1500 °C. The flexural strengths of the order of 300 MPa could be obtained, and the eutectic exhibits a fracture toughness of $3 \text{ MPm}^{0.5}$ over a wide range of processed shapes and sizes. The toughness is higher than the two constituents. The creep resistance of this eutectic is excellent up to 1500 °C which when combined with the high fracture toughness makes it the most attractive oxide system for structural use above 1200 °C. The fracture toughness is still a critical limiting factor. A systematic study of dopants to weaken the YAG-alumina phase boundary might uncover an approach to high toughness versions of this otherwise very attractive material for a wide range of applications at very high temperatures.

References

1. T. Mah, T.A. Parthasarathy, and L.E. Matson, *Ceram. Eng. Sci. Proc.* 11[9-10] (1617-1627)1990.
2. T.A. Parthasarathy, T. Mah, and L.E. Matson, *Ceram. Eng. Sci. Proc.* 11[9-10] (1990) 1628-1638.
3. T.A. Parthasarathy, T. Mah, and L.E. Matson, *J. Amer. Ceram. Soc.* 76[1] (1993) 29-32.
4. A. Sayir, and L.E. Matson, *HITEMP Review NASA CP-10082 1[83]* (1992) 1-13.
5. T. Mah, T.A. Parthasarathy, D. Petry, and L.E. Matson, *Ceram. Eng. & Sci. Proc.* 14[7-8] (1993) 622-638.
6. T. Mah, T.A. Parthasarathy, and M.D. Petry, *SBIR Phase II Final Report, WL-TR-94-4087[UES, Inc.]* (1993).
7. A. Sayir, R.M. Dickerson, H.M. Yun, S. Heideger, and L.E. Matson, *HITEMP Review NASA CP-10146 1[74]* (1994) 1-18.
8. G.N. Morscher, S. Farmer, and A. Sayir, *Ceram. Eng. & Sci. Proc.* 16[5] (1995) 959-968.
9. Y. Waku, H. Ohtsubo, N. Nakagawa, and Y. Kohtoku, *J. of Mater. Sci.* 31[17] (1996) 4663-4670.
10. Y. Waku, N. Nakagawa, T. Wakamoto, H. Ohtsubo, K. Shimuzu, and Y. Kohtoku, *J. of Mater. Sci.* 33[20] (1998) 4943-4951.
11. Y. Waku, N. Nakagawa, T. Wakamoto, H. Ohtsubo, K. Shimuzu, and Y. Kohtoku, *J. of Mater. Sci.* 33[5] (1998) 1217-1225.
12. L.E. Matson and N.L. Hecht, *Journal of the European Ceramic Society, PII: S0955-2219* (1999) 2487-2501.
13. A. Yoshikawa, K. Hasegawa, T. Fukuda, and K. Suzuki, *Cer. Eng. Sci. Proc. B* 20[4] (1999) 275-282.
14. K. Yoshida, A. Nakamura, T. Sakuma, N. Nakagawa, and Y. Waku, *Scripta Materialia* 45[8] (2001) 957-963.
15. Y. Waku, and T. Sakuma, *J. of Eur. Ceram. Soc.* 20[10] (2000) 1453-1458.
16. S. Ochiai, T. Ueda, K. Sato, M. Hojo, Y. Waku, N. Nakagawa, S. Sakata, A. Mitani, and T. Takahashi, *Comp. Sci & Tech.* 61[14] (2001) 2117-2128.
17. T. Murayama, S. Hanada, and Y. Waku, *Materials Trans.* 44[9] (2003) 1690-1693.
18. Y. Harada, T. Suzuki, K. Hirano, and Y. Waku, *J. Amer. Ceram. Soc.* 86[6] (2003) 951-958.
19. Y. Harada, T. Suzuki, K. Hirano, and Y. Waku, *J. Eur. Cer. Soc.* 24 (2004) 2215-2222.
20. G.S. Corman, *Ceram. Eng. & Sci. Proc.* 12[9-10] (1991) 1745-1767.
21. G.S. Corman, *J. Mat. Sci. Let.* 12 (1993) 379-382.
22. T.A. Parthasarathy, T. Mah, and K. Keller, *Ceram. Engr. &*

- Sci. Proc. 12[9-10] (1991) 1767-1773.
23. T.A. Parthasarathy, T.-I. Mah, and K. Keller, *J. Am. Ceram. Soc.* 75[7] (1992) 1756-1759.
 24. J.W. Halloran, R.M. Laine, B.H. King, and Y. Liu, *WL-TR-94-4100* (1994).
 25. S. Karato, Z. Wang, and K. Fujino, *J. Mat. Sci.* 29 (1994) 6458-6462.
 26. G.N. Morscher, K.C. Chen, and K.S. Mazdiyasn, *Cer. Eng. Sci. Proc.* 15[4] (1994) 181-188.
 27. T. Mah, T.A. Parthasarathy, L. Boothe, M.D. Petry, and L.E. Matson, "Directional Solidification of Refractory Oxide Ceramic Eutectic Composites" *WRDC-TR-90-4081* (1990).
 28. I. Warshaw and R. Roy, *Journal of Amer. Ceram. Soc.* 42[9] (1959) 434-438.
 29. D. Viechnicki and F. Schmid, *Jl of Mater. Sci.* 4 (1969) 84-85.
 30. J.L. Caslavsky and D. Viechnicki, *Jl of Mater. Sci.* 15 (1980) 1709-1718.
 31. T. Mah and M.D. Petry, *J. Am. Ceram. Soc.* 75[7] (1992) 2006-2009.
 32. R.S. Hay, *J. Am. Cer. Soc.* 77[6] (1994) 1473-1485.
 33. H. Yasuda, Y. Mizutani, T. Ohnaka, A. Sugiyama, T. Morikawa, and Y. Waku, *J. Amer. Ceram. Soc.* 86[10] (2003) 1818-1820.
 34. H. Yasuda, I. Ohnaka, Y. Mizutani, and Y. Waku, *Science and Techn. of Adv. Mater.* 2 (2001) 67-71.
 35. R.L. Ashbrook, *Jl of Amer. Ceram. Soc.* 60[9-10] (1977) 428-435.
 36. V.S. Stubican and R.C. Bradt, *Ann. Rev. Mater. Sci.* 11 (1981) 267-297.
 37. Z. Li and R.C. Bradt, *J. Eur. Cer. Soc.* 9[2] (1992) 143-152.
 38. E.C. Dickey, C.S. Frazer, T.R. Watkins, and C.R. Hubbard, *J. Eur. Cer. Soc.* 19 (1999) 2503-2509.
 39. S. Takata, S. Ueno, T.Y. C.J.M, Y.M, and E. Yasuda, *Int. J. Mater. & Prod. Tech.* 16[1-3] (2001) 269-275.
 40. Y. Mizutani, H. Yasuda, I. Ohnaka, N. Maeda, and Y. Waku, *J. of Crystal Growth* 244 (2002) 384-392.
 41. Y. Mizutani, H. Yasuda, I. Ohnaka, N. Maeda, and Y. Waku, *J. of the Jap. Inst. Metals* 66[1] (2002) 9-15.
 42. H. Yasuda, I. Ohnaka, Y. Mizutani, A. Sugiyama, T. Morikawa, S. Takeshima, T. Sakimura, and Y. Waku, *Science and Techn. of Adv. Mater.* 5 (2004) 207-217.
 43. A. Sayir, in *Computer Aided Design of High Temperature Materials* A. Pechenik, R. Kalia, P. Vashishta, Eds. (Oxford University Press, 1999) pp. 197-211.
 44. C.S. Frazer, E.C. Dickey, and A. Sayir, *J. of Crystal Growth* 233[1-2] (2001) 187-195.
 45. P.A. Doleman and E.G. Butler, *Key Eng. Mater.* 127-131 (1997) 193-202.
 46. B.M. Epelbaum, A. Yoshikawa, K. Shimamura, T. Fukuda, K. Suzuki, and Y. Waku, *J. of Crystal Growth* 198/199 (1999) 471-475.
 47. T. Mah, T.A. Parthasarathy, and R.J. Kerans, *Jl Amer. Ceram. Soc.* 83[8] (2000) 2088-2090.
 48. T. Isobe, M. Omori, and T. Hirai, *J. Japan. Soc. Powder and Powder Metall.* 47[3] (2000) 298-301.
 49. T. Isobe, M. Omori, S. Uchida, T. Sato, and T. Hirai, *J. Eur. Cer. Soc.* 22 (2002) 2621-2625.
 50. L.E. Matson, R.S. Hay, and T. Mah, *Cer. Eng. Sci. Proc.* 11[7-8] (1990) 995-1003.
 51. R.S. Hay and L.E. Matson, *Acta Met.* 39[8] (1991) 1981-1994.
 52. R.S. Hay, *MRS Symp. Proc.* 357 (1995) 145-151.
 53. T.A. Parthasarathy, Air Force Research Laboratory, [Unpublished Work] WPAFB, OH (1992).
 54. T. Isobe, M. Omori, and T. Hirai, *J. Cer. Soc. of Japan* 109[1] (2001) 66-70.
 55. N. Bahlawane, T. Watanabe, Y. Waku, A. Mitani, and N. Nakagawa, *J. Amer. Ceram. Soc.* 83[12] (2000) 3077-3081.
 56. A. Otsuka, Y. Waku, K. Kitagawa, and N. Arai, *J. of the Ceram. Soc. of Japan* 111[2] (2003) 87-92.
 57. D.-Y. Park, J.-M. Yang, and J.M. Collins, *J. Amer. Ceram. Soc.* 84[12] (2001) 2991-2996.
 58. J.M. Collins, J.M. Yang, and A. Sayir, AFOSR-Phase2-SBIR#F49620-96-C-0047, [Sapphikon, Inc.] (1998).
 59. S.C. Farmer, A. Sayir, R.M. Dickerson, and L.E. Matson, *Ceram. Eng. & Sci. Proc.* 21[3] (2000) 125-131.
 60. S.C. Farmer, A. Sayir, P.O. Dickerson, and S.L. Draper, *Ceram. Eng. & Sci. Proc.* 16[5] (1995) 969-975.
 61. M. Iwasa, and R.C. Bradt, in *Advances in Ceramics*. (The Amer. Cer. Soc., Columbus, OH, 1984), vol. 10, pp. 759-779.
 62. T. Mah and T.A. Parthasarathy, *Jl of the Amer. Ceram. Soc.* 80[10] (1997) 2730-2734.
 63. K. Hirano, T. Suzuki, A. Kamei, and F. Tamai, *Int. J. Mater. & Prod. Tech.* 16[1-3] (2001) 276-283.
 64. K. Hirano, Y. Unno, Y. Harada, and M. Kikuchi, *Key Eng. Mater.* 243-244 (2003) 33-38.
 65. J.E. Pitchford, F. Deleglise, M.H. Berger, A.R. Bunsell, and W.J. Clegg, *Ceram. Eng. & Sci. Proc.* 22[3] (2001) 415-420.
 66. M. Miyazaki, N. Ikeda, and T. Komura, *J. of Eng. Mater. Tech., Trans. of the ASME* 125[3] (2003) 277-282.
 67. H. Yoshida, K. Shimura, S. Suginozawa, Y. Ikuhara, T. Sakuma, N. Nakagawa, and Y. Waku, *Key Eng. Mater.* 171-174 (2000) 855-862.
 68. S. Sambasivan, T.A. Parthasarathy, F.J. Scheltens, and R.J. Kerans, *Cer. Eng. Sci. Proc.* 14[9-10] (1993) 873-877.
 69. T. Mah and T.A. Parthasarathy, unpublished work, [Wright-Patterson AFB OH] (1999).
 70. D.Y. Park and J.M. Yang, *Mater. Sci. & Eng.* 332[1-2] (2002) 276-284.
 71. L.N. Brewer, D.P. Endler, B.S. Austin, V.P. Dravid, and J.M. Collins, *J. Mater. Res. Soc.* 14[10] (1999) 3907-3912.
 72. Y. Waku, N. Nakagawa, T. Wakamoto, H. Ohtsubo, K. Shimizu, and Y. Kohtoku, *Nature* 389[49-52] (1997).
 73. N. Nakagawa, Y. Waku, and T. Wakamoto, *Mater. & Man. Proc.* 115[5] (2000) 709-725.
 74. M. Fernandez, A. Sayir, M. Singh, and T. Jesson, *Cer. Eng. Sci. Proc.* 22[3] (2001) 421-428.
 75. J.M. Fernandez, A. Sayir, and S.C. Farmer, *Acta Mater.* 51[6] (2003) 1705-1720.
 76. T. Mah and T.A. Parthasarathy, *Scripta Metall. et Materialia* 28 (1993) 1383-1385.
 77. T.A. Parthasarathy, M.G. Mendiratta, and D.M. Dimiduk, *Scripta Mater.* 37[3] (1997) 315-321.
 78. W.S. Walston, K.S. Ohara, E.W. Ross, T.M. Pollock, and W.H. Murphy, *Rene N6: Third Generation Single Crystal Superalloy*, R.D. Kissinger *et al.*, Eds., *Superalloys 1996* (The Minerals, Metals and Materials Society, 1996).
 79. A.D. Cetel and D.N. Duhl, *Second-Generation Nickel-Base Single Crystal Superalloy*, S. Reichman, D.N. Duhl, G. Maurer, S. Antolovich, C. Lund, Eds., *Superalloys 1988* (The Metallurgical Society, 1988).
 80. T.A. Parthasarathy and R.S. Hay, *Jl of the Amer. Ceram. Soc.* 44[12] (1996) 4663-4676.
 81. D.M. Kotchik and R.E. Tressler, *J. Amer. Ceram. Soc.* 63[7-8] (1980) 429-437.
 82. J.E. Lane, C.H. Carter, and R.F. Davis, *J. Amer. Ceram. Soc.* 71[4] (1988) 281-295.